

Chaos in hyperscaling violating Lifshitz theories

Nikesh Lilani^{1,*}

¹*Department of Physics and Astronomy, National Institute of Technology Rourkela, Rourkela - 769008, India*

Abstract

We holographically study quantum chaos in hyperscaling-violating Lifshitz (HVL) theories (with charge). Specifically, we present a detailed computation of the out-of-time ordered correlator (OTOC) via shockwave analysis in the bulk HVL geometry with a planar horizon topology. We also compute the butterfly velocity (v_B) using the entanglement wedge reconstruction and find that it matches the result obtained from the shockwave analysis. Using a recently developed thermodynamic dictionary for HVL theories, we express v_B purely in terms of boundary thermodynamic variables. Furthermore, we analyze in detail the behavior of v_B with respect to the dynamical critical exponent (z), hyperscaling-violating parameter (θ), entropy (more precisely, the ratio of entropy to the central charge, \tilde{S}), and charge (more precisely, the ratio of charge to the central charge, \tilde{Q}). Interestingly, v_B varies non-monotonically with z for $\tilde{S} < 1$, whereas it increases monotonically with z for $\tilde{S} \geq 1$. Additionally, v_B varies non-monotonically with θ for non-zero charge. Moreover, v_B monotonically increases with \tilde{S} and decreases with \tilde{Q} for all allowed values of z and θ . All these features are reported for combinations $\{z, \theta, \tilde{S}, \tilde{Q}\}$ for which the temperature is positive, the null energy condition is satisfied, and v_B is not superluminal. Unpacking the non-monotonicities in v_B can offer interesting insights into these theories.

I Introduction

Chaos is present in a large class of physical systems that generally exhibit sensitive dependence on initial conditions. Tools of chaos theory are used in a plethora of works ranging from the small quantum domain [1] to the large-scale structures in spacetime [2].

Classically, chaos is characterized by an exponential divergence between two phase space trajectories, with the Lyapunov exponent λ_L parametrizing the rate of this divergence. However, characterization of quantum chaos is a lot more challenging, because the sensitivity in initial conditions cannot be directly computed due to the uncertainty principle. Initially, characterization of quantum chaos

* imnikeshlilani@gmail.com

was based on comparison between the system's spectrum of energies and the spectrum of random matrices [3]. However, a new approach was developed in [4] (in the context of semi-classical systems) and [5]. Quantum chaos can be characterized by the strength of the commutator between two generic operators V and W separated by time t . To be precise, the following quantity is considered: $\langle -[W(t), V(0)]^2 \rangle_\beta$, where expectation value is taken in the thermal state β . One can also consider the spreading of chaos in spatial directions, by taking the two operators to be also spatially separated. In such a case, the commutator is given by (15), where v_B is the butterfly velocity. Roughly speaking, v_B characterizes the rate at which the information about the applied perturbation "spreads" (or scrambles among the local degrees of freedom) in the system (this notion is made precise in III). Focus is laid on v_B in this work.

Gauge/gravity duality ([6], [7]) is the idea that a gravitational theory in a $(d+1)$ dimensional bulk spacetime is dual to a d dimensional quantum theory (without gravity) residing at the asymptotic boundary of the bulk spacetime. AdS/CFT correspondence [8–10] is the most well understood realization of this duality. In the framework of AdS/CFT correspondence, a gravitational theory in asymptotically AdS spacetime in the bulk is dual to a conformal field theory (CFT). However, the general principles of gauge/gravity duality can be extended to bulk spacetimes that are not asymptotically AdS and equivalently boundary theories that are not conformally invariant. Lifshitz theories are an example of such theories that are not conformally invariant. These theories exhibit an anisotropic scaling symmetry between space and time, parametrized by the dynamical critical exponent z , i.e. $\{t, x\} \rightarrow \{\alpha^z t, \alpha x\}$. Theories with $z \neq 1$ do not support Lorentz invariance and instead possess non-relativistic symmetries. Also, for $z \neq 1$, these theories describe quantum critical systems (non-relativistic). Bulk gravitational theory dual to Lifshitz theory was first proposed in [11]. (see also [12–16]). The anisotropic scaling symmetry of the boundary theory can be geometrically realized in the bulk via these so-called Lifshitz spacetimes.

Quantum critical point may be characterized by several other critical exponents that satisfy certain relations and thereby are dependent on each other. Hyperscaling relations are a certain class of critical exponent relations in which there is an explicit appearance of dimensionality of the space [17]. There are critical theories that violate this hyperscaling relation. For such theories the heat capacity $C_v \sim T^{(d-1-\theta)/z}$ ([18],[19]), where θ is called the hyperscaling-violating parameter. Essentially, θ reduces the effective dimensionality of the theory. For hyperscaling-violating and Lifshitz (HVL) theories, the dual bulk black hole solutions have been obtained in several works [20–25]. In this paper, we closely follow the discussion in [25].

In recent years, the study of chaotic dynamics of strongly-coupled many-body quantum systems via gauge-gravity duality has witnessed a significant interest [26–29]. For a comprehensive review of holographic chaos, refer [30]. Through [31], it was established that black holes are the fastest scramblers in nature. Thus, in the context of AdS/CFT, the rapid thermalization of a local perturbation in the boundary CFT is understood through the fast scrambling dynamics of a black hole in the bulk. It is also known that black holes in holography can be characterized via quantum chaos [31], [32]. Possessing maximal chaos is thought of as a criterion for a QFT to have a gravity dual [8], [26], [33].

In this work, we holographically study quantum chaos in HVL theories (with charge). In particular, we compute the out-of-time-ordered correlator (OTOC) (we make the notion precise in III) via shockwave analysis in the bulk geometry (for planar horizon topology) and thereby compute the various chaos parameters, namely the Lyapunov exponent (λ_L), butterfly velocity (v_B) and the scrambling time (t_*) for the HVL theories. One of the motivations for studying OTOCs in HVL theories is the recent proposals for experimentally measuring OTOCs in quantum systems [34–37]. We also compute v_B using the entanglement wedge reconstruction and find the results obtained from both the methods, to match. Furthermore, we study how boundary thermodynamics and theory parameters (z and θ) affect information scrambling. To achieve this, we use a recently developed thermodynamic dictionary for the HVL theories [38] to express v_B in terms of boundary thermodynamic variables. We study the variation of v_B with respect to the theory parameters z and θ , as well as the boundary thermodynamic variables: entropy over central charge ($\tilde{S} \sim S/C$) and charge over central charge ($\tilde{Q} \sim Q/C$). Several interesting features are obtained.

The structure of this paper is as follows: In II, we discuss the charged hyperscaling-violating Lifshitz black hole solution and also discuss the constraints on z and θ that arise from the null-energy condition. In III, we provide a detailed analysis of computing the OTOC for HVL theories via the shockwave analysis. In IV, we compute v_B using the entanglement wedge reconstruction and find the results of III and IV to match. In V, we discuss the thermodynamic dictionary and express v_B in terms of the boundary thermodynamic variables. In VI, we discuss the variation of v_B with respect to the various z , θ , \tilde{S} , and \tilde{Q} . We conclude in VII.

II Background

In this paper, we follow the discussion in [25]. The HVL black hole solution obtained in [25] is a generalization of charged black brane solutions with arbitrary z and θ (of [20]) to other topologies

(namely spherical and hyperbolic).

The line element is given as follows

$$ds^2 = \left(\frac{r}{r_F}\right)^{\frac{-2\theta}{d-1}} \left[-\left(\frac{r}{L}\right)^{2z} f(r) dt^2 + \frac{L^2}{f(r)r^2} dr^2 + r^2 d\Omega_{k,d-1}^2 \right] \quad (1)$$

where $f(r)$ is the blackening function given as

$$f(r) = 1 + k \frac{(d-2)^2}{(d-\theta+z-3)^2} \frac{L^2}{r^2} - \left(\frac{r_h}{r}\right)^{d-\theta+z-1} \left[1 + k \frac{(d-2)^2}{(d-\theta+z-3)^2} \frac{L^2}{r_h^2} + \frac{q^2}{r_h^{2(d-\theta+z-2)}} \right] + \frac{q^2}{r^{2(d-\theta+z-2)}} \quad (2)$$

r_h is the horizon radius, d is the number of boundary dimensions, q is the charge parameter, k is the factor that characterizes the topology of the horizon ($k = \{-1, 0, 1\}$ for hyperbolic, planar and spherical horizon topology respectively), r_F is the large radius upto which the black hole geometry is considered to be valid, (r_F corresponds to the UV cutoff scale in the boundary), and L is the bulk curvature radius. The temperature can be computed from the blackening function.

$$T = \frac{f'(r_h)}{4\pi} \left(\frac{r_h}{L}\right)^{z+1} = \frac{r_h^z}{4\pi L^{z+1}} \left[d - \theta + z - 1 + \frac{k(d-2)^2}{d-\theta+z-3} \frac{L^2}{r_h^2} - \frac{(d-\theta+z-3)q^2}{r_h^{2(d-\theta+z-2)}} \right] \quad (3)$$

The charged and static black hole solutions given by (1) were analytically constructed from the following generalized Einstein-Maxwell-Dilaton (EMD) action

$$S = -\frac{1}{16\pi G} \int d^{d+1}x \sqrt{-g} \left[R - \frac{1}{2}(\nabla\phi)^2 + V(\phi) - \frac{1}{4}X(\phi)F^2 - \frac{1}{4}Y(\phi)H^2 - \frac{1}{4}Z(\phi)K^2 \right] \quad (4)$$

Here F , H and K are the field strengths corresponding to the three Abelian gauge fields A, B, C , given as $F = dA$, $H = dB$ and $K = dC$. ϕ is a real scalar field known as the dilaton field. X , Y and Z are the respective coupling functions of the gauge fields and the dilaton field given as

$$X = X_o e^{\lambda_1 \phi}, \quad Y = Y_o e^{\lambda_2 \phi}, \quad Z = Z_o e^{\lambda_3 \phi} \quad (5)$$

Here, X_o , Y_o , and Z_o are positive parameters that quantify the strength of coupling between gravity and the three gauge fields respectively, and λ_i 's are constants given as

$$\lambda_1 = \frac{-2(d-1-\theta+\theta/(d-1))}{\tilde{\gamma}}, \quad \lambda_2 = \frac{-2(d-2)(d-\theta-1)}{\tilde{\gamma}(d-1)}, \quad \lambda_3 = \frac{\tilde{\gamma}}{d-\theta-1} \quad (6)$$

where $\tilde{\gamma}$ is given as

$$\tilde{\gamma} = \sqrt{2(d-\theta-1) \left(z - 1 - \frac{\theta}{d-1} \right)} \quad (7)$$

Note that the gauge field A supports the Lifshitz asymptotics, B supports the other non-planar horizon topologies (hyperbolic and spherical) and C allows for a non-zero electric charge. In this work we

deal only with planar horizon topology ($k = 0$) and set $L = 1$. For $k = 0$ and $L = 1$, $f(r)$ and temperature are given as

$$f(r) = 1 - \left(\frac{r_h}{r}\right)^{d-\theta+z-1} \left[1 + \frac{q^2}{r_h^{2(d-\theta+z-2)}} \right] + \frac{q^2}{r^{2(d-\theta+z-2)}} \quad (8)$$

$$T = \frac{r_h^z}{4\pi} \left[d - \theta + z - 1 - \frac{(d - \theta + z - 3)q^2}{r_h^{2(d-\theta+z-2)}} \right] \quad (9)$$

A Constraints on z and θ

It is assumed that the null energy condition serves as a sufficient condition to have a physically consistent holographic dual in the semi-classical limit. The requirement of satisfying the null energy condition imposes certain constraints on z and θ . The null energy condition is given as

$$T_{\mu\nu}\xi^\mu\xi^\nu \geq 0 \quad (10)$$

or equivalently,

$$R_{\mu\nu}\xi^\mu\xi^\nu \geq 0 \quad (11)$$

where ξ^μ is a null vector. Considering two orthogonal null vectors, we obtain the following two inequalities from (11) (for $k = 0$)

$$(d - 1 - \theta)((d - 1)(z - 1) - \theta) \geq 0 \quad (12)$$

$$\frac{r^2}{(z - 1)(d - 1 - \theta + z)} + \frac{q^2(d - 1 - \theta)((d - 1)(z - 1) - \theta)}{r^{2(d - 1 - \theta + z - 2)}} \geq 0 \quad (13)$$

Note that the black hole solution is only valid for $\theta < d - 1$ and $d - \theta + z - 3 > 0$. Combining these inequalities with (12) and (13), we get the following constraints on the values of z and θ for $k = 0$.

$$z < 1 \implies \text{no solution}$$

$$1 \leq z < 2 \implies \text{solution exists for } \theta \leq (d - 1)(z - 1) \quad (14)$$

$$z \geq 2 \implies \text{solution exists for } \theta < d - 1$$

These constraints play an important role in the discussion in VI.

III Out-of-time ordered correlator (OTOC)

For two spatially separated generic Hermitian operators V and W , quantum chaos can be characterized by the following commutator $[W(0, -t), V(x, 0)]$. Note that, since it is of interest to study thermal systems, an expectation value of the commutator is taken in a thermal state β . However, the thermal expectation value may attain a negative sign which can thereby lead to cancellations. To overcome this, the commutator is squared and thus the precise quantity to be considered, is the following.

$$C(x, t) = \langle -[W(0, -t), V(x, 0)]^2 \rangle_{\beta} \quad (15)$$

where the overall minus sign is introduced to make $C(x, t)$ positive. $C(x, t)$ characterizes the strength of the effect that the perturbation W at an earlier time $-t$ and $x = 0$ has, on the measurement of the operator V at $t = 0$ and at a spatial point x . We choose to work with past time ($-t$) because it is convenient when we consider the holographic picture. (15) can be expanded as follows.

$$C(x, t) = 2 - \langle W(0, -t)V(x, 0)W(0, -t)V(x, 0) \rangle \quad (16)$$

The second term in (16) is called the out-of-time ordered correlator (OTOC) (simply because the operators are not time-ordered). The vanishing of the OTOC is considered as a diagnostic of chaos in a physical system. This can be realized by considering the following two states.

$$|\psi_1\rangle = W(0, -t)V(x, 0)|\beta\rangle \quad (17)$$

$$|\psi_2\rangle = V(x, 0)W(0, -t)|\beta\rangle \quad (18)$$

OTOC is the overlap between the above two states. The state $|\psi_1\rangle$ can be physically described as follows: at time $t = 0$ (and at spatial point x), the state $V(x, 0)|\beta\rangle$ is prepared. The state is then evolved backward in time, a small perturbation W is applied, and the state is evolved forward in time again. If the perturbation W is applied sufficiently early in the past, and the system is chaotic (i.e., highly sensitive to initial conditions), the operator V will fail to reappear at $t = 0$. On the other hand, the state $|\psi_2\rangle$ is understood as follows: a perturbation W is applied at time $-t$, and then the system is evolved in such a way that the operator V appears at $t = 0$. For chaotic systems, the overlap between the two states $|\psi_1\rangle$ and $|\psi_2\rangle$ vanishes. As a result, OTOC vanishes, leading to the growth of the commutator, as is evident from equation (16). In the case of conformal field theories (CFTs) and higher-dimensional SYK models, this commutator between two spatially separated operators shows

exponential growth.

$$C(x,t) \sim \exp \left[\lambda_L \left(t - t_* - \frac{|x|}{v_B} \right) \right] \quad (19)$$

Here, λ_L is the quantum Lyapunaov exponent, t_* is the scrambling time and v_B is the butterfly velocity. The scrambling time t_* is defined as the time at which the commutator with $x = 0$ becomes order unity. In chaotic systems, the commutator with $x = 0$ exhibits an exponential growth upto the scrambling time. After the scrambling time, the information about a local perturbation starts scrambling among the local degrees of freedom at a constant rate, characterized by the butterfly velocity v_B . After time t of inserting the perturbation operator W ($|t| > |t_*|$), the commutator is order unity in the region given by ($|x| < v_B|t - t_*|$), and this region is said to be the "size" of the operator W (it is the region in which the measurement of any operator is significantly affected by W).

A Kruskal extension and the shockwave analysis

In this subsection, we compute the various chaos parameters for HVL theories via the shockwave analysis in the bulk. It is standard to work with the two-sided eternal black hole geometry, which corresponds to a thermo-field double state (denoted as $|TFD\rangle$) in the boundary. Note that we will consider planar horizon topology (i.e. $k = 0$) for our analysis throughout.

In order to work in the two-sided geometry, the metric (1) is written in the Kruskal co-ordinates. The Kruskal co-ordinate transformation is given as

$$u = \exp \left[\frac{2\pi}{\beta} (r_* - t) \right], \quad v = -\exp \left[\frac{2\pi}{\beta} (r_* + t) \right] \quad (20)$$

Where, β is the inverse Hawking temperature and r_* is the tortoise co-ordinate.

$$dr_* = \frac{dr(r^{z+1})}{f(r)} \quad (21)$$

In the Kruskal co-ordinates the metric takes the following form

$$ds^2 = 2A(u,v)dudv + B(u,v)dx^i dx^j \quad (22)$$

where $A(u,v)$ and $B(u,v)$ are related to the blackening function as follows.

$$A(u,v) = \frac{f[r(u,v)] [r(u,v)]^{2(z-\frac{\theta}{d-1})}}{(2\alpha^2 uv) r_F^{\frac{-2\theta}{d-1}}}; \quad B(u,v) = \frac{[r(u,v)]^{2(1-\frac{\theta}{d-1})}}{r_F^{\frac{-2\theta}{d-1}}} \quad (23)$$

Here $\alpha = \frac{2\pi}{\beta}$. In order to know the explicit expressions of A and B in terms of u and v, we need to find $r[u, v]$. (21) is not integrable. However, as we shall discuss, the shockwave is localized at the horizon and thus we deal with the near-horizon limit. The integral given by (21), can be expanded around the horizon. The dominating term in the expansion is the logarithmic term given as.

$$r_* \approx \frac{1}{f'(r_h)r_h^{z+1}} \log(r - r_h) \quad (24)$$

Multiply u and v, given by (20), we get the following.

$$uv = -e^{2\alpha r_*} = -e^{4\pi T z_*} \quad (25)$$

Substituting (24), (3) in (25), we get the following.

$$r = r_h - uv \quad (26)$$

Putting $u = 0$ or $v = 0$, we get that $r = r_h$. This implies that $u = 0$ and $v = 0$ are the two horizons of the two-sided geometry (as is the case in Kruskal co-ordinates). Substituting (26) in (23), we get the explicit form of A and B in terms of the Kruskal co-ordinates (u and v).

Now, we compute the OTOC. In the framework of AdS/CFT, each operator \hat{Q} in the boundary corresponds to a scalar perturbation $\phi(x, t)$ in the bulk. Consider acting an operator $W(0, -t)$ on $|TFD\rangle$ in the right boundary. In the two-sided black hole geometry, this corresponds to a particle coming out from the past interior, reaching the boundary at time $-t$ and then falling towards the future interior. The energy of the particle falling into the black hole increases exponentially and it depends on the temperature of the black hole.

$$E = E_o e^{\frac{2\pi}{\beta} t} \quad (27)$$

Here E_o is the energy of the particle when it's near the boundary. Since, the energy of the particle gets exponentially blue-shifted, a sufficiently earlier perturbation in the boundary, $W(0, -t)$, leads to a non-trivial modification of the bulk geometry. The large energy of the particle leads to a back reaction in the geometry, which simply corresponds to a shockwave geometry [27]. The energy distribution of this perturbation is compressed along u and stretched along v. Thus, for sufficiently large time $|t|$, the perturbation gets localized along the horizon $u = 0$ (refer figure 1) and, the stress energy tensor attains the following form.

$$T_{uu}^{shock} = E_o e^{\frac{2\pi}{\beta} t} \delta(u) a(x) \quad (28)$$

Where $a(x)$ is some function to be determined. The effect of this shock, localized along the horizon

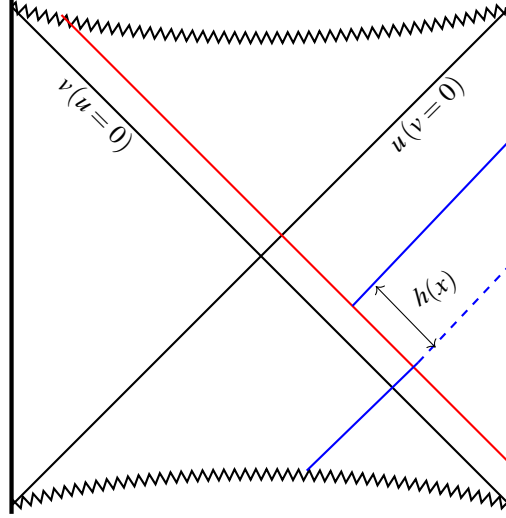


FIG. 1: The Penrose diagram, explaining the effect of the shockwave created near the horizon. The red line represents the shockwave created by the perturbation particle W , which is inserted at a sufficiently earlier time. In the absence of the shockwave, particle V would have emerged from the past interior and would have reached the boundary at $t = 0$. However, due to the shockwave, the V particle suffers a shift in its trajectory, which is parametrized by $h(x)$. This causes a delay in the appearance of operator V at the boundary. If the W perturbation is applied early enough (i.e., $|t| \gtrsim |t_*|$), the trajectory of the particle gets shifted to the point that it gets engulfed by the future interior and the V particle fails to reach the boundary altogether.

$u = 0$ is that the particle coming from the past interior suffers a shift in the trajectory (refer figure), which is given as

$$v \rightarrow v + \Theta(u)h(x), \quad u \rightarrow u \quad (29)$$

Here, the step function $\Theta(u)$ accounts for the fact that the causal future of the particle is affected after it encounters the horizon $u = 0$ (and thus there's no affect on the causal past). $h(x,t)$ is a function that characterizes the amount of shift and it is to be determined by the Einstein equation. To understand the relation between this function $h(x,t)$ and the commutator (and thereby the OTOC), consider the bulk picture of the two states $|\psi_1\rangle$ and $|\psi_2\rangle$. The bulk picture of $|\psi_1\rangle$ is as follows: Initially, the system is prepared in such a way that the V particle from the past interior reaches the boundary at $t = 0$. However, the insertion of the operator W at a sufficiently earlier time makes the particle encounter a localized shock at the horizon, which results in the shift of particle's trajectory, which in turn, causes a time delay in the appearance of the operator V at the boundary. On the other hand, the state $|\psi_2\rangle$ corresponds to the V particle reaching the boundary at $t = 0$, "after" suffering the shift due to the

shock. Thus, the overlap between the two states (and thus the OTOC) keeps decreasing for earlier and earlier times. After a certain past time, the shift suffered by the particle is such that the particle gets trapped inside the future interior and then it cannot escape to the boundary, making the overlap and thus the OTOC completely vanish. This time is given by the scrambling time, $|t| \gtrsim |t_*|$.

The shift in the co-ordinates (29) results in the following modified metric.

$$ds^2 = 2A(u, v)dudv + B(u, v)dx^2 - 2A(u, v)h(x, t)\delta(u)du^2 \quad (30)$$

The total stress tensor is now given as

$$T = T_o + T^{shock} \quad (31)$$

Here, T_o is the initial unperturbed stress tensor and the only non-zero component of T^{shock} is given by (28). Substituting (31) and (30) in the Einstein equation and solving for the uu component, we arrive at the following.

$$\left(\partial_i \partial_i - \frac{d-1}{2} \frac{\partial_u \partial_v B}{A} \right) h(x) \delta(u) = \frac{8\pi G_N E_o B}{A} e^{\frac{2u}{\beta}} \delta(u) a(x) \quad (32)$$

For large x , ($|x| \gg 1$), the function $a(x)$ can be replaced by the Dirac delta function, because the solution depends only on the integral of $a(x)$. Solving for large x , we get the following solution for $h(x)$

$$h(x) = \frac{e^{\frac{2\pi}{\beta}(t-t_*) - \chi|x|}}{|x|^{\frac{d-2}{2}}} \quad (33)$$

Where χ and t_* are given as

$$\chi = \sqrt{\frac{d-1}{2} \left(\frac{\partial_u \partial_v B(0)}{A(0)} \right)} \quad (34)$$

$$t_* = \frac{2\pi}{\beta} \log \left(\frac{A(0)}{8\pi G_N E_o B(0)} \right) \quad (35)$$

where $\partial_u \partial_v B(0)$ denotes the double derivative of B evaluated at the horizon and $A(0)$, $B(0)$ denote the functions A and B, evaluated at the horizon. Comparing (33) with (19), we can read off the butterfly velocity and the Lyapunov exponent.

$$v_B = \frac{2\pi}{\beta\chi} \quad (36)$$

$$\lambda_L = 2\pi T \quad (37)$$

We can compute v_B and t_* by evaluating the values of A, B and $\partial_u \partial_v B$ at the horizon $u = 0$. Note that, at the horizon, A attains a $\frac{0}{0}$ form. Thus we compute the limit of A as $u \rightarrow 0$, which is well defined.

The required horizon-limit values are

$$A(0) = \lim_{u \rightarrow 0} A = \frac{r_h^{-1-2d} \left(\frac{r_h}{r_F}\right)^{-\frac{2\theta}{d-1}} \left(-r_h^{2(d+z)}(d-1+z-\theta) - q^2 r_h^{4+2\theta}(3-d-z+\theta)\right)}{2\alpha^2} \quad (38)$$

$$B(0) = \left(\frac{r_h}{r_F}\right)^{-\frac{2\theta}{d-1}} r_h^2 \quad (39)$$

$$\partial_u \partial_v B(0) = \frac{-2r_h \left(\frac{r_h}{r_F}\right)^{-\frac{2\theta}{d-1}} + 2r_h^2 \left(\frac{r_h}{r_F}\right)^{-1-\frac{2\theta}{d-1}} \theta}{(d-1)r_F} \quad (40)$$

Using (38), (39), (40), and (3) (for $k = 0$) we can compute the three chaos parameters for the HVL theories. .

$$t_* = \frac{1}{2} r_h^{1+z} \left(-2q^2 r_h^{3-2d-2z+2\theta} (d-2+z-\theta) + (1+q^2) \left(\frac{1}{r_h}\right)^{d+z-\theta} (d-1+z-\theta) \right) \times \log \left(\frac{\left(r_h^{2(d+z)}(1-d-z+\theta) + q^2 r_h^{4+2\theta}(d-3+z-\theta)\right)}{4G_N \pi E_o r_h^5 \left(-2q^2 r_h^{3-d-z+2\theta}(d-2+z-\theta) + (1+q^2) r_h^\theta (d-1+z-\theta)\right)^2} \right) \quad (41)$$

$$v_B^2 = \frac{r_h^{2(z-1)}(d-1+z-\theta) + q^2 r_h^{-2(d-1-\theta)}(3-d-z+\theta)}{2(d-1-\theta)} \quad (42)$$

$$\lambda_L = \frac{r_h^z}{2} \left[d - \theta + z - 1 - \frac{(d - \theta + z - 3)q^2}{r_h^{2(d-\theta+z-2)}} \right] \quad (43)$$

For $r_h = 1$, the expressions for these parameters become simpler.

$$t_* = \frac{1}{2} (d-1+z-\theta + q^2(3-d-z+\theta)) \log \left(\frac{1}{4G_N \pi E_o (1-d-z+\theta - q^2(3-d-z+\theta))} \right) \quad (44)$$

$$v_B^2 = \frac{d-1+z-\theta + q^2(3-z+\theta-d)}{2(d-1-\theta)} \quad (45)$$

$$\lambda_L = \frac{1}{2} (-1+d+z-\theta + q^2(3-d-z+\theta)) \quad (46)$$

Note that for $\theta = 0$, $r_h = 1$, and $q = 0$, the result (42) matches the result obtained in [39]. Also, as an important sidenote, we point out that the butterfly velocity (42) is equal to the velocity of entanglement growth during thermalization at the saturation point ¹ (for $q = 0$) [40], suggesting an interesting connection between the two notions.

¹ Author would like to thank Mohammad Reza Mohammadi Mozaffar for pointing this out.

IV Entanglement wedge

In this section, we compute v_B using another method, namely the entanglement wedge method. Through the works [41–44], it was established that a certain sub-region A on the boundary is dual to the entanglement wedge in the bulk. The entanglement wedge is the region in the bulk, bounded by the sub-region A and the extremal surface homologous to A. In [45], it was shown that the butterfly velocity (for isotropic and planar bulk geometries) can be computed using the entanglement wedge reconstruction.

Consider some perturbation in the boundary theory. As time passes, the information from the perturbation gets delocalized over a larger and larger region, i.e. the size of the applied operator increases. The size of the operator is the smallest region that contains the information of the applied perturbation operator. In the dual bulk picture, it corresponds to the extremal surface "just" enclosing the particle (i.e. the particle is at the tip of the extremal surface at all times) (refer figure 2). It's important to note that the background geometry is static and it's only the position of the particle that is time-dependent. So the RT surface [46] is used as the extremal surface and not the HRT surface [47]. Thus, in this case the entanglement wedge is a constant t hyper-surface, bounded by the RT surface and the boundary sub-region.

The area functional (or equivalently, the entanglement entropy functional) is given as follows.

$$S_{EE} = 2\pi \int \sqrt{\gamma} d^{d-1} \xi \quad (47)$$

Here γ is the determinant of the induced metric on the co-dimension 2 surface in the bulk and ξ are the co-ordinates on the surface. Extremising the above action (or equivalently the induced metric) will give rise to the equation of the RT surface. So we first compute the induced metric on the surface. Since the surface is embedded in a $t = \text{constant}$ hypersurface, the tt component of the induced metric vanishes. Further, taking \tilde{r} to be the radial co-ordinate in the x^i direction ($\tilde{r} = |x|$) and parametrizing r with \tilde{r} ($r = r(\tilde{r})$), we get the following induced metric from (1)

$$\gamma_{ab} d\xi^a d\xi^b = \left[\frac{(z')^2 \left(\frac{r}{r_F}\right)^{-\frac{2\theta}{d-1}}}{r^2 f(r)} + \left(\frac{r}{r_F}\right)^{-\frac{2\theta}{d-1}} r^2 \right] d\tilde{r}^2 + \left[\left(\frac{r}{r_F}\right)^{-\frac{2\theta}{d-1}} r^2 \right] \tilde{r}^2 d\Omega_{0,d-2}^2 \quad (48)$$

In order to compute the butterfly velocity, a near-horizon analysis of the RT surface is done (refer figure 2). Near the horizon, the following form of $r(\tilde{r})$ can be taken.

$$r(\tilde{r}) = 1 - \epsilon u(\tilde{r})^2 \quad (49)$$

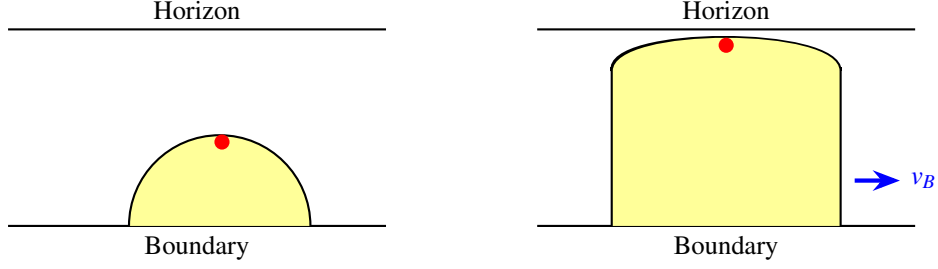


FIG. 2: The growth of the entanglement wedge (shaded in yellow) as the particle, originating from the boundary (represented by the red dot), propagates towards the horizon. The figure on the left shows the entanglement wedge at some time t and the figure on the right shows the entanglement wedge at a sufficiently later time t' , when the RT surface reaches near the horizon and the near-horizon profile of the RT surface is given by $u(\tilde{r})$.

For simplicity, here we have taken the horizon radius $r_h = 1$, ε is some arbitrarily small parameter and $u(\tilde{r})$ is the function to be determined by extremizing (47). Substituting (49) in the induced metric and expanding near the horizon, upto $O(\varepsilon)$, we get the following.

$$\sqrt{\gamma} = r_F^\theta \tilde{r}^{d-2} \left(1 - \varepsilon \frac{\left(4r_F^{\frac{2\theta}{d-1}} (u')^2 + (d-1)u^2 f_o' \left(2r_F^{\frac{2\theta}{d-1}} \left[1 - \frac{\theta}{d-1} \right] \right) \right)}{2r_F^{\frac{2\theta}{d-1}} f_o'} \right) \quad (50)$$

Here f_o' represents the derivative of the blackening function, evaluated at the horizon. Extremising (50) (and thereby S_{EE}) we arrive at the following differential equation in $u(\tilde{r})$.

$$u''(\tilde{r}) + (d-2) \frac{u'(\tilde{r})}{\tilde{r}} - \frac{f_o'}{2} (d-1-\theta) u(\tilde{r}) = 0 \quad (51)$$

The RT surface starts to depart the near-horizon region for large \tilde{r} . To put it precisely, the RT surface stays close to the horizon up to the point where $\varepsilon u(\tilde{r})^2 \sim O(1)$, and after that, the surface departs the near horizon region and reaches the boundary to order one distance. As suggested in [48], we can encapsulate this behaviour via the following ansatz.

$$u(\tilde{r}) \sim \frac{e^{\mu\tilde{r}}}{\tilde{r}^n} \quad (52)$$

where n is some positive integer. Also, the particle touches the tip of the RT surface at all times. Hence, taking the tip of the RT surface to be the origin, we can set $u(0, t) \sim e^{-\frac{2\pi t}{\beta}}$. Thus $u(\tilde{r}, t)$ is given as follows.

$$u(\tilde{r}, t) \sim \frac{e^{\mu\tilde{r} - \frac{2\pi t}{\beta}}}{\tilde{r}^n} \quad (53)$$

The rate at which the particle propagates towards the horizon is the rate at which the size of the applied operator grows. Thus, from (53), the butterfly velocity is given as.

$$v_B = \frac{2\pi}{\beta\mu} \quad (54)$$

To determine v_B , we need to determine μ . To determine μ , we substitute the ansatz (52) in (51). Dropping higher order terms in $1/\tilde{r}$, we get the following expression for μ .

$$\mu^2 = \frac{f'_o}{2}(d-1-\theta) \quad (55)$$

Substituting (55) and (9) in (54), we get the following expression for the butterfly velocity.

$$v_B^2 = \frac{d-1+z-\theta+q^2(3-z+\theta-d)}{2(d-1-\theta)} \quad (56)$$

The above result matches the result obtained via the shockwave analysis (45).

V v_B in terms of the boundary thermodynamic variables

The next goal is to understand how boundary thermodynamics and theory parameters (θ and z) affect information scrambling in HVL theories. In order to achieve that goal, we first express v_B (given by (42)) purely in terms of boundary thermodynamic variables, using a recently developed thermodynamic dictionary for HVL theories [38]. This dictionary has various merits, such as the matching of the Smarr formula on the bulk side with the Euler relation on the boundary side, as well as the matching of the first laws on the boundary and in the bulk. Here, we list the dictionary entries that are relevant for expressing v_B in terms of the boundary thermodynamics. The entries for central charge, entropy, and charge are as follows

$$C = \frac{\Omega_{k,d-1} L^{d-\theta-1} r_F^\theta}{16\pi G_N} \quad (57)$$

$$S = 4\pi C x^{d-\theta-1} \quad (58)$$

$$Q = \sqrt{2Z_o} C q [(d-\theta-1)(d-\theta+z-3)]^{\frac{1}{2}} \quad (59)$$

Here, x is a bulk parameter given as $x \equiv \frac{r_h}{L}$ and S and Q are dimensionless. Note that, in none of the relevant entries (for our purposes), is there an appearance of the arbitrary length parameter r_o (refer

[38]) and thus there is no effect of r_o on how information scrambles in the boundary. We continue working with $L = 1$ (and $k = 0$). r_h and q are the two bulk parameters that we need to eliminate in (42) and thus we express these parameters in terms of the boundary quantities in the following way.

$$r_h = \tilde{S}^{\frac{1}{d-\theta-1}} \quad (60)$$

$$q = \frac{\tilde{Q}}{[(d-\theta-1)(d-\theta+z-3)]^{1/2}} \quad (61)$$

where \tilde{S} and \tilde{Q} are defined as

$$\tilde{S} \equiv \frac{S}{4\pi C} \quad (62)$$

$$\tilde{Q} \equiv \frac{Q}{\sqrt{2Z_o C}} \quad (63)$$

Substituting (60) and (61) in (42), we get the following expression for v_B in terms of the boundary thermodynamic variables.

$$v_B^2 = \frac{\tilde{S}^{\frac{2(z-1)}{d-\theta-1}} (d-1+z-\theta)(d-\theta-1) - (\tilde{Q}/\tilde{S})^2}{2(d-\theta-1)^2} \quad (64)$$

We treat Z_o as a constant parameter. It is interesting to note that the entropy couples to both z and θ , however charge does not couple to z . With the expression (64) in hand, we now study the variation of v_B with respect to z , θ , \tilde{S} and \tilde{Q} .

VI Variation of v_B with z , θ , \tilde{S} and \tilde{Q}

In this section, we study the variation of v_B and note some interesting features. Before proceeding, there are certain important points to highlight. Given that the Lorentz invariance is broken in HVL theories, v_B is not bounded by v_B^S [45], where v_B^S is the butterfly velocity for AdS-Schwarzschild black brane, given as

$$v_B^S = \sqrt{\frac{d}{2(d-1)}} \quad (65)$$

and is, moreover, super-luminal for certain values of the parameters. Secondly, in this section, we only deal with the "permissible" values of the parameters and thermodynamic variables, where by permissible we mean the combination $\{z, \theta, \tilde{S}, \tilde{Q}\}$ for which the temperature $T > 0$. Furthermore,

we also keep track of the constraints on z and θ imposed by the null energy condition, discussed in [II A](#). For analysis in this section, we fix $d = 4$.

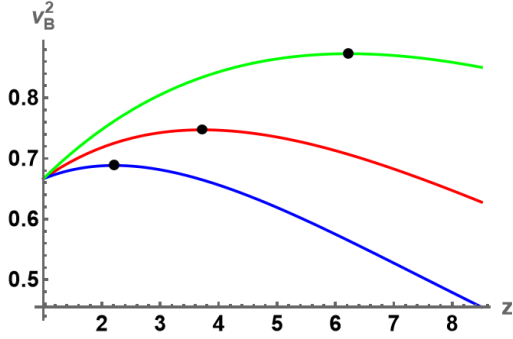
First, to analyze only the effect of z , we set $\theta = 0$ (i.e. purely Lifshitz theories). Initially, we deal with the case where $\tilde{Q} = 0$ and then consider the effect of non-zero charge. For $\theta = 0$ and $\tilde{Q} = 0$, v_B interestingly exhibits non-monotonic behavior with respect to z when $0 < \tilde{S} < 1$, in the permissible region. We get a maxima. However, only in the range $0.688 < \tilde{S} < 0.877$, the non-monotonicities lie in the allowed region for z , i.e. ($z > 1$) and v_B at the non-monotonic point is not superluminal. Since the charge does not couple to z , there is no non-trivial effect of non-zero \tilde{Q} . $\tilde{Q} \neq 0$ merely shifts the values and does not change the behavior of v_B with respect to z . For $\tilde{S} \geq 1$, v_B monotonically increases with z in the permissible region. This suggests that v_B does not necessarily increase with z in Lifshitz theories, as reported in earlier works (such as [\[39\]](#)), but it depends on entropy per central charge.

Next, to study the effect of θ , we set $z = 1$ (i.e. purely hyperscaling-violating theories). For $z = 1$, the corresponding constraint on θ is $\theta \leq 0$. We divide the discussion into two subcases $\tilde{Q} = 0$ and $\tilde{Q} \neq 0$. For $z = 1$ and $\tilde{Q} = 0$, v_B monotonically increases with θ for all values of \tilde{S} . However, since charge couples with θ , the effect of non-zero charge is non-trivial. $\tilde{Q} \neq 0$ induces a non-monotonicity in v_B when varied with respect to θ . We get a maxima (again, we mean in the permissible region, for allowed values of θ with v_B not being superluminal).

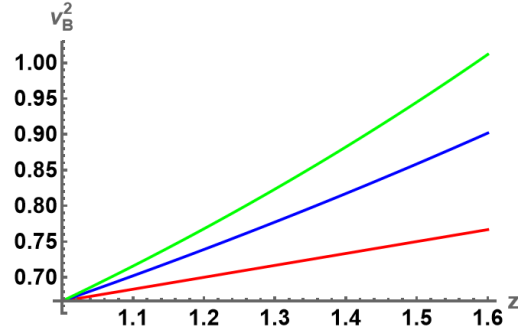
It is important to note that the non-monotonicities in v_B , as a function of z and θ , do not coincide with those in temperature. This can be verified by plotting T and v_B on the same graph. Hence, the underlying causes of the non-monotonicities in v_B and temperature are not the same.

With respect to \tilde{S} , v_B increases monotonically in the permissible region and for all allowed values of z and θ . Note that the entropy dependence of v_B arises due to the appearance of r_h in [\(36\)](#). However, v_B is a model-dependent parameter, and in certain holographic models, r_h does not appear in the expression for v_B . In such models, entropy does not affect information scrambling. One example of this is the planar RNAdS black hole.

On the other hand, v_B monotonically decreases with respect to \tilde{Q} (by which we mean the magnitude of the charge) in the permissible region and for all allowed values of z and θ . It is interesting to note that, in one of the author's upcoming works, quantum chaos in a completely different class of holographic models has been studied, and it is found that v_B necessarily depends on charge and moreover, in all the models studied in the work, v_B is found to monotonically decrease with charge (or more precisely, the magnitude of the charge). This observation suggests that the slowing down of

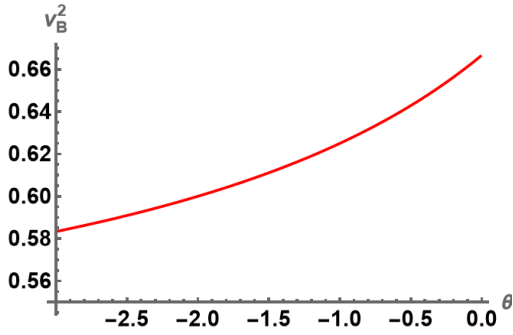


(a) $\tilde{S} < 1$, $\tilde{Q} = 0$, $\theta = 0$, and $d = 4$ for this plot. The blue, red and green curves correspond to $\tilde{S} = 0.7$, $\tilde{S} = 0.75$ and $\tilde{S} = 0.8$ respectively. The black dots represent the non-monotonocities.

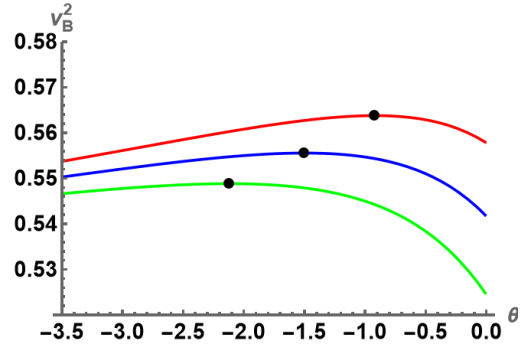


(b) $\tilde{S} \geq 1$, $\tilde{Q} = 0$, $\theta = 0$, and $d = 4$ for this plot. The red, blue and green curves correspond to $\tilde{S} = 1$, $\tilde{S} = 1.5$ and $\tilde{S} = 2$ respectively.

FIG. 3: v_B^2 vs z

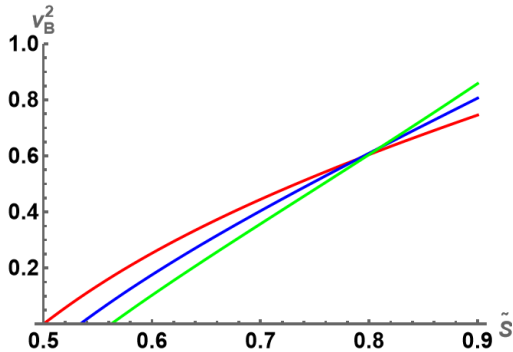


(a) $\tilde{Q} = 0$, $z = 1$, and $d = 4$ for this plot. The plot is the same for all values of \tilde{S} .

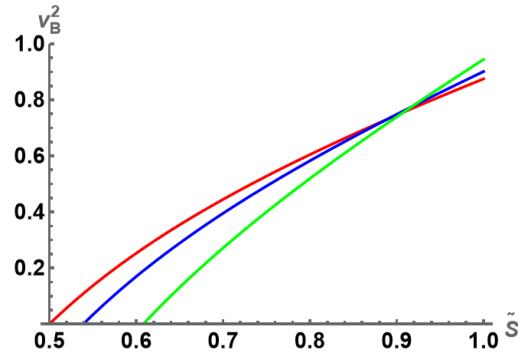


(b) $\tilde{Q} \neq 0$, $z = 1$, $\tilde{S} = 1$ and $d = 4$ for this plot. The red, blue, and green curves correspond to $\tilde{Q} = 1.4$, $\tilde{Q} = 1.5$ and $\tilde{Q} = 1.6$. The black dots represent the non-monotonocities.

FIG. 4: v_B^2 vs θ

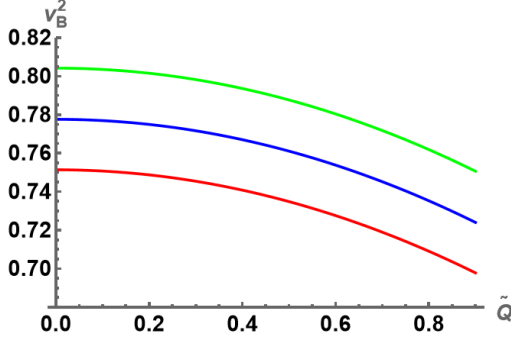


(a) $\tilde{Q} = 1$, $\theta = 1$, and $d = 4$ for this plot. The green, blue and the red curves correspond to $z = 3$, $z = 2.5$, and $z = 2$ respectively.

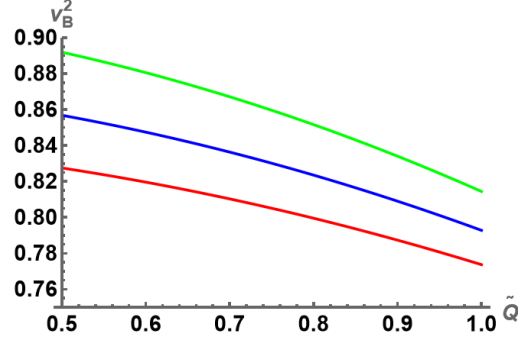


(b) $\tilde{Q} = 1$, $z = 2$, and $d = 4$ for this plot. The green, blue and the red curves correspond to $\theta = 1.5$, $\theta = 1.2$, and $\theta = 1$ respectively.

FIG. 5: v_B^2 vs \tilde{S}

(a) $\tilde{S} = 1.1$, $\theta = 0.5$, and $d = 4$ for this plot.

The red, blue and green curves correspond to $z = 1.2$, $z = 1.3$, and $z = 1.4$ respectively.

(b) $\tilde{S} = 1.1$, $z = 1.5$, and $d = 4$ for this plot.

The red, blue and green curves correspond to $\theta = 0.6$, $\theta = 0.8$, and $\theta = 1$ respectively.

FIG. 6: v_B^2 vs \tilde{Q}

the rate of information scrambling by charge might be a universal feature of all holographic models or even a characteristic of all quantum systems in general.

VII Discussion and future outlook

In this work, we presented a detailed discussion on the shockwave analysis in HVL theories and computed various chaos parameters. v_B was also computed using the entanglement wedge method, and the results obtained from both methods were found to match. Note that our analysis was restricted to planar horizon topology. One can extend the analysis to hyperbolic and spherical topologies and analyze what effect a non-zero k has on the behavior of v_B . However, this task would require devising certain new methods.

Furthermore, using a recently developed thermodynamic dictionary, we expressed v_B purely in terms of boundary thermodynamics, which yielded a neat result. We then discussed the variations of v_B with respect to z , θ , \tilde{S} , and \tilde{Q} . Notably, we observed a non-monotonic behavior of v_B when varied with respect to z for $\tilde{S} < 1$, whereas v_B was found to increase monotonically with z for $\tilde{S} \geq 1$. This implies that z does not necessarily increase v_B (as reported in previous works [39]). This suggests that entropy non-trivially affects the rate of information scrambling. Thus, to gain deeper insights into the nature of information scrambling in any holographic model, it is more useful to retain r_h in the expression of v_B (instead of setting it equal to one, as is commonly practiced in the literature).

In uncharged hyperscaling-violating theories, v_B was found to increase monotonically with θ ,

whereas for non-zero charge, a non-monotonic behavior was obtained. Additionally, v_B was observed to increase monotonically with \tilde{S} and decrease monotonically with \tilde{Q} . The latter fact also holds for a completely different class of holographic models discussed in one of the author's upcoming works, and thus one can conjecture that charge decreases the rate of information scrambling in all holographic models or quantum systems in general. It would be interesting to investigate whether a counter-example to this conjecture exists.

When varying z or θ , one navigates through a space of theories. The observed non-monotonicities suggest that the theories on either side of the non-monotonic points may possess distinguishing features, leading to different natures of information scrambling on either side. Unpacking the underlying physics behind these non-monotonicities (as well as other features discussed) is an interesting direction for future work. Additionally, we noted that v_B equals the rate of entanglement growth during thermalization, indicating a connection between the two, which would also be an interesting avenue to explore further.

VIII Acknowledgements

NL would like to sincerely thank Subhash Mahapatra for his invaluable guidance and fruitful discussions, Siddhi Swarup Jena for helping with the two figures and Bhaskar Shukla for important discussions. NL would also like to thank Michael Blake, Victor Jahnke, Mohammad Reza Mohammadi Mozaffar, Douglas Stanford, and Marika Taylor for their useful comments and suggestions.

-
- [1] M. Srednicki, *Chaos and Quantum Thermalization*, *Phys. Rev. E* **50** (1994) [[cond-mat/9403051](#)].
 - [2] S. Suzuki and K.-i. Maeda, *Chaos in Schwarzschild space-time: The motion of a spinning particle*, *Phys. Rev. D* **55** (1997) 4848 [[gr-qc/9604020](#)].
 - [3] D. Ullmo and S. Tomsovic, *Introduction to quantum chaos*, 2012, <https://api.semanticscholar.org/CorpusID:49572714>.
 - [4] A.I. Larkin and Y.N. Ovchinnikov, *Quasiclassical Method in the Theory of Superconductivity*, *Soviet Journal of Experimental and Theoretical Physics* **28** (1969) 1200.
 - [5] A. Almheiri, D. Marolf, J. Polchinski, D. Stanford and J. Sully, *An Apologia for Firewalls*, *JHEP* **09** (2013) 018 [[1304.6483](#)].
 - [6] G. 't Hooft, *Dimensional reduction in quantum gravity*, *Conf. Proc. C* **930308** (1993) 284 [[gr-qc/9310026](#)].
 - [7] L. Susskind, *The World as a hologram*, *J. Math. Phys.* **36** (1995) 6377 [[hep-th/9409089](#)].

- [8] J.M. Maldacena, *The Large N limit of superconformal field theories and supergravity*, *Adv. Theor. Math. Phys.* **2** (1998) 231 [[hep-th/9711200](#)].
- [9] E. Witten, *Anti-de Sitter space and holography*, *Adv. Theor. Math. Phys.* **2** (1998) 253 [[hep-th/9802150](#)].
- [10] S.S. Gubser, I.R. Klebanov and A.M. Polyakov, *Gauge theory correlators from noncritical string theory*, *Phys. Lett. B* **428** (1998) 105 [[hep-th/9802109](#)].
- [11] S. Kachru, X. Liu and M. Mulligan, *Gravity duals of lifshitz-like fixed points*, *Physical Review D* **78** (2008) .
- [12] K. Balasubramanian and J. McGreevy, *Gravity duals for non-relativistic CFTs*, *Phys. Rev. Lett.* **101** (2008) 061601 [[0804.4053](#)].
- [13] M. Taylor, *Non-relativistic holography*, [0812.0530](#).
- [14] E. Ayón-Beato, A. Garbarz, G. Giribet and M. Hassaïne, *Lifshitz black hole in three dimensions*, *Physical Review D* **80** (2009) .
- [15] R.B. Mann, *Lifshitz Topological Black Holes*, *JHEP* **06** (2009) 075 [[0905.1136](#)].
- [16] G. Bertoldi, B.A. Burrington and A. Peet, *Black Holes in asymptotically Lifshitz spacetimes with arbitrary critical exponent*, *Phys. Rev. D* **80** (2009) 126003 [[0905.3183](#)].
- [17] B. Widom, *Surface tension and molecular correlations near the critical point*, *Journal of Chemical Physics* **43** (1965) 3892.
- [18] B. Gouteraux and E. Kiritsis, *Generalized Holographic Quantum Criticality at Finite Density*, *JHEP* **12** (2011) 036 [[1107.2116](#)].
- [19] L. Huijse, S. Sachdev and B. Swingle, *Hidden Fermi surfaces in compressible states of gauge-gravity duality*, *Phys. Rev. B* **85** (2012) 035121 [[1112.0573](#)].
- [20] M. Alishahiha, E. O Colgain and H. Yavartanoo, *Charged Black Branes with Hyperscaling Violating Factor*, *JHEP* **11** (2012) 137 [[1209.3946](#)].
- [21] X. Dong, S. Harrison, S. Kachru, G. Torroba and H. Wang, *Aspects of holography for theories with hyperscaling violation*, *JHEP* **06** (2012) 041 [[1201.1905](#)].
- [22] B. Gouteraux and E. Kiritsis, *Quantum critical lines in holographic phases with (un)broken symmetry*, *JHEP* **04** (2013) 053 [[1212.2625](#)].
- [23] J. Gath, J. Hartong, R. Monteiro and N. Obers, *Holographic models for theories with hyperscaling violation*, *Journal of High Energy Physics* **2013** (2012) .
- [24] P. Bueno, W. Chemissany and C. Shahbazi, *On hvlf-like solutions in gauged supergravity*, *The European Physical Journal C* **74** (2012) .
- [25] J.F. Pedraza, W. Sybesma and M.R. Visser, *Hyperscaling violating black holes with spherical and hyperbolic horizons*, *Class. Quant. Grav.* **36** (2019) 054002 [[1807.09770](#)].
- [26] S.H. Shenker and D. Stanford, *Black holes and the butterfly effect*, *Journal of High Energy Physics* **2014** (2014) .

- [27] D.A. Roberts, D. Stanford and L. Susskind, *Localized shocks*, *Journal of High Energy Physics* **2015** (2015) .
- [28] D.A. Roberts and B. Swingle, *Lieb-robinson bound and the butterfly effect in quantum field theories*, *Phys. Rev. Lett.* **117** (2016) 091602.
- [29] E. Perlmutter, *Bounding the Space of Holographic CFTs with Chaos*, *JHEP* **10** (2016) 069 [1602.08272].
- [30] V. Jahnke, *Recent developments in the holographic description of quantum chaos*, *Adv. High Energy Phys.* **2019** (2019) 9632708 [1811.06949].
- [31] Y. Sekino and L. Susskind, *Fast scramblers*, *Journal of High Energy Physics* **2008** (2008) 065–065.
- [32] J.M. Maldacena, *Eternal black holes in anti-de Sitter*, *JHEP* **04** (2003) 021 [hep-th/0106112].
- [33] S.H. Shenker and D. Stanford, *Stringy effects in scrambling*, *JHEP* **05** (2015) 132 [1412.6087].
- [34] B. Swingle, G. Bentsen, M. Schleier-Smith and P. Hayden, *Measuring the scrambling of quantum information*, *Phys. Rev. A* **94** (2016) 040302.
- [35] G. Zhu, M. Hafezi and T. Grover, *Measurement of many-body chaos using a quantum clock*, *Phys. Rev. A* **94** (2016) 062329.
- [36] J. Li, R. Fan, H. Wang, B. Ye, B. Zeng, H. Zhai et al., *Measuring out-of-time-order correlators on a nuclear magnetic resonance quantum simulator*, *Phys. Rev. X* **7** (2017) 031011.
- [37] N.Y. Yao, F. Grusdt, B. Swingle, M.D. Lukin, D.M. Stamper-Kurn, J.E. Moore et al., *Interferometric Approach to Probing Fast Scrambling*, 1607.01801.
- [38] W. Cong, D. Kubizňák, R.B. Mann and M.R. Visser, *Holographic dictionary for Lifshitz and hyperscaling violating black holes*, 2410.16145.
- [39] B. Baishya, A. Chakraborty and N. Padhi, *A study of three butterflies: entanglement wedge method, OTOC and pole-skipping*, 2406.18319.
- [40] M. Alishahiha, A. Faraji Astaneh and M.R. Mohammadi Mozaffar, *Thermalization in backgrounds with hyperscaling violating factor*, *Phys. Rev. D* **90** (2014) 046004 [1401.2807].
- [41] B. Czech, J.L. Karczmarek, F. Nogueira and M. Van Raamsdonk, *The Gravity Dual of a Density Matrix*, *Class. Quant. Grav.* **29** (2012) 155009 [1204.1330].
- [42] A.C. Wall, *Maximin Surfaces, and the Strong Subadditivity of the Covariant Holographic Entanglement Entropy*, *Class. Quant. Grav.* **31** (2014) 225007 [1211.3494].
- [43] M. Headrick, V.E. Hubeny, A. Lawrence and M. Rangamani, *Causality & holographic entanglement entropy*, *JHEP* **12** (2014) 162 [1408.6300].
- [44] X. Dong, D. Harlow and A.C. Wall, *Reconstruction of Bulk Operators within the Entanglement Wedge in Gauge-Gravity Duality*, *Phys. Rev. Lett.* **117** (2016) 021601 [1601.05416].
- [45] M. Mezei and D. Stanford, *On entanglement spreading in chaotic systems*, *JHEP* **05** (2017) 065 [1608.05101].
- [46] S. Ryu and T. Takayanagi, *Holographic derivation of entanglement entropy from the anti-de sitter space/conformal field theory correspondence*, *Physical Review Letters* **96** (2006) .

- [47] V.E. Hubeny, M. Rangamani and T. Takayanagi, *A Covariant holographic entanglement entropy proposal*, *JHEP* **07** (2007) 062 [0705.0016].
- [48] X. Dong, D. Wang, W.W. Weng and C.-H. Wu, *A tale of two butterflies: an exact equivalence in higher-derivative gravity*, *Journal of High Energy Physics* **2022** (2022) .